A compact dual-circularly polarized cavity-backed ring-slot antenna

Riaan Ferreira, Johan Joubert, *Senior Member IEEE*, and Johann W. Odendaal, *Senior Member IEEE*

***Abstract*— A low profile dual-circularly polarized printed ring-slot antenna with a small footprint, which radiates above an open cavity loaded with an artificial magnetic conducting (AMC) reflector, is presented. The feed network consists of two T-shaped capacitive feed structures connected to a miniaturized hybrid branch-line coupler. Experimental results for a final antenna design (with a size of $0.5\lambda_0 \times 0.5\lambda_0 \times 0.057\lambda_0$) show a 4% isolation bandwidth between the two ports of the dual-circularly polarized antenna and a maximum gain of approximately 6.8 dBic. Good front-to-back ratios and low cross-polarization were achieved. This very compact and low profile antennas are suitable for 2.4 GHz wireless local area network communication systems.**

***Index Terms*—Cavity backed antennas, circular polarization, electromagnetic bandgap materials, microstrip couplers, slot antennas.**

I. INTRODUCTION

Circularly polarized antennas are commonly used in applications such as radio frequency identification (RFID), radar tracking and satellite communication systems. The use of circularly polarized antennas is useful in these applications since it can reduce multi-path interferences and allows for flexible alignments between the transmitter and receiver antennas [1].

Slot antennas can be used for portable units and unobtrusive base stations if you can succeed in making the antennas small and low profile. A conventional printed slot antenna will radiate bi-directionally. A variety of techniques are available to achieve uni-directional radiation of a printed slot radiator [2-5]. One such method is to place an electric conducting reflector below the slot. The typical distance to place such an electric reflector is a quarter of a wavelength [2, 3], resulting in antennas that have quite substantial heights. It is possible to use a smaller spacing between the antenna and electric ground plane, but impedance matching of the antenna may become a problem if the spacing is too small.

In order to make the uni-directional slot radiators more compact, an artificial magnetic conducting (AMC) reflector can be placed close to the radiator [4, 5]. Elek et al [4] published results for a uni-directional ring-slot antenna and focused on finding a suitable electromagnetic band-gap (EBG) surface to minimize radiation leakage between the parallel plates of the structure. They opted to use the popular "mushroom" periodic surface proposed by Sievenpiper et al in [6]. The work in [4] showed that the inclusion of the EBG surface dramatically suppressed the propagation of the unwanted TEM-mode between the plates. The EBG surface that is closely spaced (much closer than a quarter-wavelength) to the ground plane in which the ring-slot is cut also acts as an AMC reflector, which allows for a low profile structure with uni-directional radiation. Joubert et al. [5] published results for a cavity backed rectangular slot radiator loaded with a closely spaced AMC reflector. A single layer patch structure was used for the unit cell of the AMC. This work shows that the energy leakage from the open cavity can be minimized if the cavity dimensions (the upper and lower cavity surfaces are respectively the AMC reflector ground plane and the slot radiator ground plane) are optimized.

Jiang et al. [7] published results for a very compact printed monopole radiating above an AMC reflector. The AMC reflector that was used had a "dog bone" like structure, and is only suitable for a single linear polarization. The final dimensions of this antenna were $0.5\lambda_0 \times 0.3\lambda_0 \times 0.028\lambda_0$. It achieved an impedance bandwidth of 5.5%, front-to-back ratio of 25 dB and cross-polarization discrimination better than 20 dB. It might be possible to extend this structure and use two monopoles, a clever feeding structure, and of course a different AMC reflector to achieve circular polarization or dual-circular polarization, but it will definitely increase the size of the antenna.

This paper presents results of a compact ring-slot radiator above an open cavity loaded with a metamaterial-based AMC surface as a reflector. The proposed antenna is a novel extension of the single polarized antennas proposed in [5, 8] to obtain a dual-circularly polarized ring-slot radiator backed by an AMC reflector. The structure of the AMC reflector consists of a patch array. The patch structure was chosen because it is known to be polarization invariant [9]. The two capacitive feeds are connected to a branch-line coupler in order to produce dual-circular polarization. The reduced size branch-line coupler proposed by Joubert et al. [10] was used and placed over the center conductor of the ring-slot and was fed with two coaxial lines through the back of the cavity. Antenna matching was achieved using a capacitive feed network as proposed in [11].

The end result and contribution of the research presented in this paper is a very low profile and small footprint antenna with reasonable gain and bandwidth, with two ports for dual-circular polarization operation, and very good front-to-back ratio and cross-polarization. To the authors' knowledge this is the smallest antenna published up to date that has a suitable bandwidth for use in 2.4 GHz wireless local area network (WLAN) communication systems. The proposed antenna is also the first dual-circularly polarized antenna for which a metamaterial reflector has been used to achieve a compact and unidirectional antenna. The new antenna has a smaller footprint than most previously published dual-polarized antennas [1, 12-14], and a better front-to-back ratio than any of the previously published works [1, 12-15].

II. ANTENNA GEOMETRY AND DESIGN

The geometry of the dual-circularly polarized ring-slot antenna radiating above an open cavity loaded with an AMC reflector is shown in Fig 1. It was designed to operate in the WLAN frequency band (2.4 – 2.484 GHz). The design was performed using CST Microwave Studio™ [16]. The radiating

R. Ferreira, J. Joubert and J.W. Odendaal are with the Centre for Electromagnetism, University of Pretoria, Pretoria 0002, South Africa (e-mail: rferreira@ymail.com, jjoubert@up.ac.za, wimpie.odendaal@up.ac.za).

slot element substrate was chosen as Rogers RO4003, with ε_r = 3.38, tan δ = 0.0021 and t_1 = 0.813 mm.

The microstripline branch-line coupler proposed in [10] was placed on top of the center conductor of the ring-slot plane, to feed the two T-shaped capacitive microstrip feedlines from the inside of the slot. A conventional branch-line coupler for this substrate would have a diameter of around 27 mm, which is too large to fit in the available space, and hence a miniaturized version of such a coupler had to be used. Two coaxial cables were used to feed the microstripline inputs to the coupler. The center conductors of the coaxial lines were connected to the microstripline feeds of the coupler and the outer conductors were connected to the center conductor of the ring-slot (to act as ground plane for the microstripline coupler). The coaxial lines were fed through two holes drilled through the AMC reflector. SUCOFORM SM 86 coaxial cables were used.

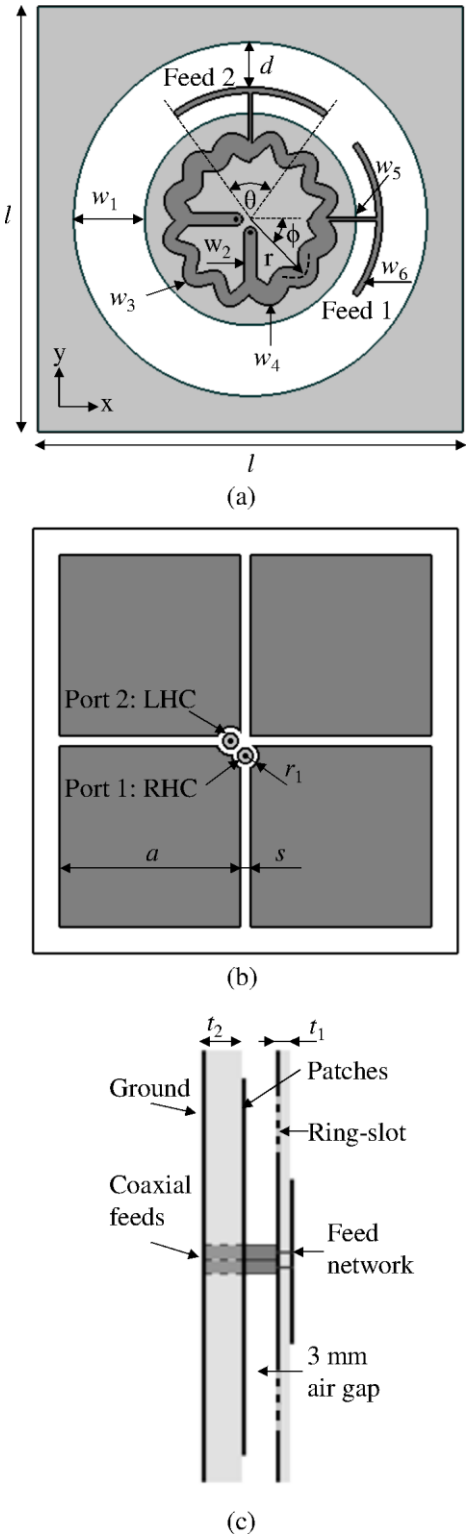

Fig. 1: Printed dual-circular ring-slot antenna above an AMC reflector: (a) top view of ring-slot, and (b) top view of AMC, (c) side view of structure.

The design process involved determining the optimum cavity dimension, choosing the slot width, and then an optimization process for the slot length and feed parameters to achieve impedance matching of the antenna. The slot length is defined as the radial circumference at the center of the slot width.

The basic AMC reflector structure consisted of 2 × 2 array of patches spaced 3.0 mm below the radiating element. An optimum rectangular cavity dimension l = 60 mm was determined using the EBG performance test as described in [5].

The unit cell dimensions of the AMC reflector was determined by using the equations in [9]. The height of the substrate t_2 primarily controls the bandwidth of the AMC reflector and was chosen as 3.048 mm in order to have a ±45° reflection phase bandwidth of 5.5%. The dimensions a and s was chosen as 25.5 mm and 1.5 mm, respectively, in order for the structure to resonate at 2.45 GHz. The inside corners of some of the AMC patches were slightly modified because an open gap (r_1 = 1.6 mm) was etched to electrically isolate the outer coaxial cable conductor from the AMC patches.

The first step in the design process was to design a dual-feed antenna (without the 90° hybrid coupler, but with dual microstripline-fed capacitive feeds from the inside of the slot). When choosing the slot width it was found that when the width is increased the impedance bandwidth increases, although when the width is too large, the isolation, front-to-back ratio and cross-polarization deteriorates. The slot width of w_1 = 10 mm was found to be a good trade-off. The next step was to go through an optimization process to find the slot length and capacitive feed parameters to achieve good impedance match and isolation between the two ports. The optimized dimensions of the capacitive feed network are as follows: w_5 = 0.45 mm, w_6 = 0.88 mm, d = 6.29 mm, θ = 70°, and the optimum slot length was 125.3 mm. The simulated S-parameters of the antenna are shown in Fig. 2, with a bandwidth of approximately 4.8% over which the reflection coefficient is better than -10 dB, and the isolation between the ports better than 12 dB.

Numerical investigation showed that an unequal 90° hybrid coupler is required for the best axial ratio results. It was found that a 1.4 dB difference in magnitude between the two input ports of the dual-feed antenna is optimum. For RHC polarization the phase and magnitude difference between capacitive feeds 1 and 2 should be 90° and -1.4 dB (for LHC -90° and 1.4 dB). The branch-line coupler was designed to achieve the desired coupling with a return loss and isolation better than 15 dB across the bandwidth of interest. The polar curves proposed in [10] were used to construct the branch-line coupler. The radial length from the center of the ring-slot structure to the middle of the curved microstrip line as a function of ϕ is described in (1). r_x is the minimum radius of the function. The constants B_1 and B_2 are the amplitudes of the

sinusoids for the low impedance and high impedance lines respectively. The final dimensions for the branch-line coupler are as follows: w_2 = 1.75 mm, w_3 = 1.86 mm, w_4 = 2.86 mm, r_x = 9.5 mm, B_1 = 0.79 mm, and B_2 = 1.13 mm. The S-parameters of the designed coupler is shown in Fig. 3. The amplitude and phase difference is shown in Fig. 4.

$$r(\phi) = \begin{cases} r_x + B_1(1-\cos(12\phi)), \phi \in [0°, 90°] \cup [180°, 270°] \\ r_x + B_2(1-\cos(12\phi)), \phi \in [90°, 180°] \cup [270°, 360°] \end{cases} \quad (1)$$

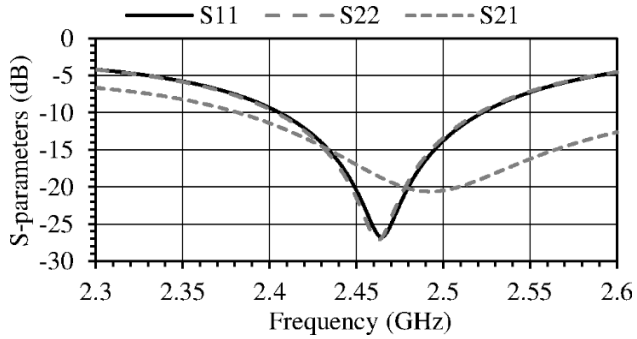

Fig. 2: S-parameters of the antenna without the coupler. Ports 1 and 2 were placed at the feed lines of the capacitive feeds 1 and 2 respectively.

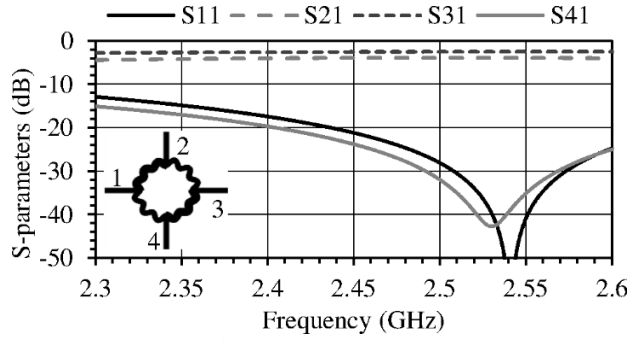

Fig. 3: S-parameters of the branch-line coupler. The structure was fed with 50 Ω microstrip lines.

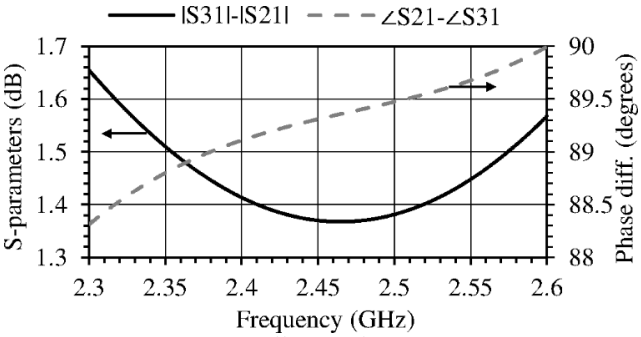

Fig. 4: Amplitude and phase difference of the branch-line coupler.

III. RESULTS

The proposed antenna was manufactured and measured to validate the theory. The manufactured prototype showed optimum isolation between the two ports at 2.4 GHz. The antenna was experimentally tuned, using copper tape, by effectively increasing angle θ for both the ports. Before tuning the measured isolation had a minimum of 20 dB at 2.4 GHz, for the tuned antenna the optimum isolation shifted to 2.423 GHz. The manufactured prototype is shown in Fig. 5.

A comparison between the simulated and measured S-parameters of the antenna is shown in Fig. 6. A 10 dB isolation bandwidth of 4% was achieved. The measured return loss of the two ports differed somewhat from each other, but still better than 10 dB across an almost 12% bandwidth.

Figs. 7 and 8 show the radiation patterns for port 1 and port 2 in the XZ-plane and the YZ-plane. A front-to-back ratio better than 30 dB and a cross-polarization discrimination of 18 dB were achieved. The measured cross-polarization differs somewhat from the simulated results, although the maximum cross-polarization discrimination only differs by 2 dB. The measured axial ratio is shown in Fig. 9. A measured 3 dB axial ratio was achieved over a beam width of 164°. The measured axial ratio was better than 3 dB over a bandwidth of 4.8%, as seen in Fig. 10. The simulated and measured gain of the antenna is also shown in Fig. 10. A maximum gain of 7.4 dBic and 6.8 dBic were respectively measured for port 1 and port 2. A measured gain of better than 6.3 dBic was achieved across the 4% isolation bandwidth. A gain improvement of 3 dB is observed when comparing this antenna to the case where the reflector is removed and the feed dimensions and slot length were adjusted to resonate at the center frequency. The isolation bandwidth can be improved by improving the impedance bandwidth at the two capacitive feed structures, which can be achieved by increasing the height t_2 of the AMC reflector.

A comparison with results achieved by other dual-circularly polarized antennas is presented in Table I. From the table, it is clear that the newly proposed antenna has a significantly better front-to-back ratio, and a good gain and reasonable bandwidth for its size. Note that the fractional bandwidth in Table I was defined as the bandwidth over which the return loss and isolation were better than 10 dB, as well as an axial ratio better than 3 dB.

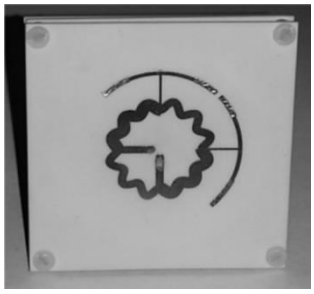

Fig. 5: Manufactured prototype of the dual-feed antenna.

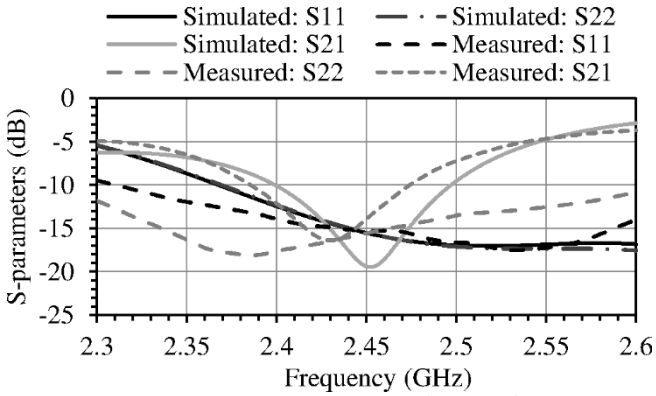

Fig. 6: Simulated and measured S-parameters of the dual-feed antenna.

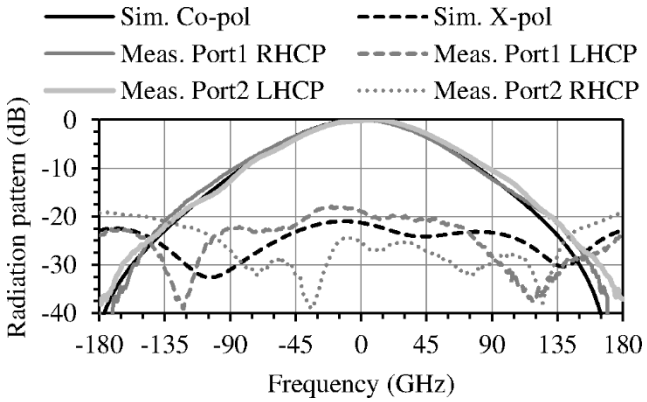

Fig. 7: Simulated and measured radiation patterns at 2.45 GHz, where Port 1 and Port2 were measured in the XZ-plane and the YZ-plane, respectively.

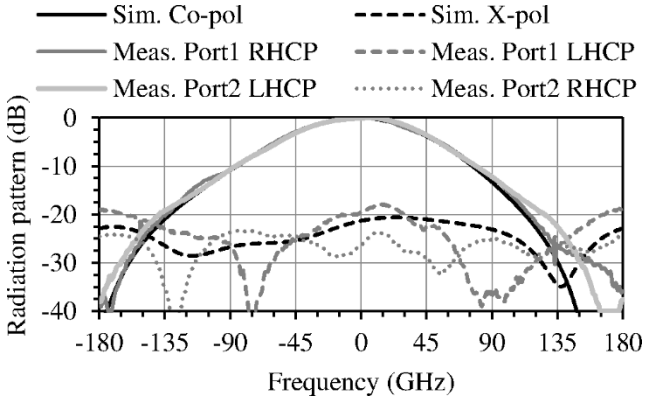

Fig. 8: Simulated and measured radiation patterns at 2.45 GHz, where Port 1 and Port2 were measured in the YZ-plane and the XZ-plane, respectively.

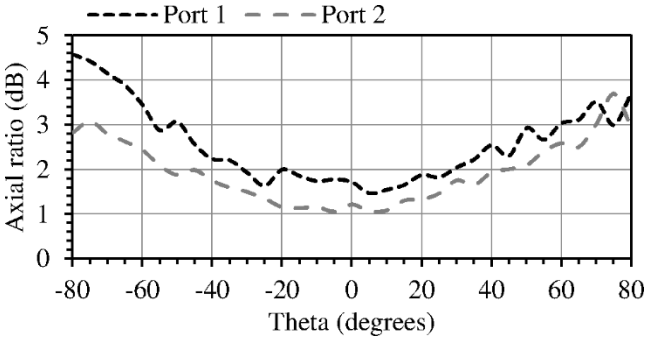

Fig. 9: Measured axial ratio at 2.45 GHz of the dual-feed antenna in the YZ-plane.

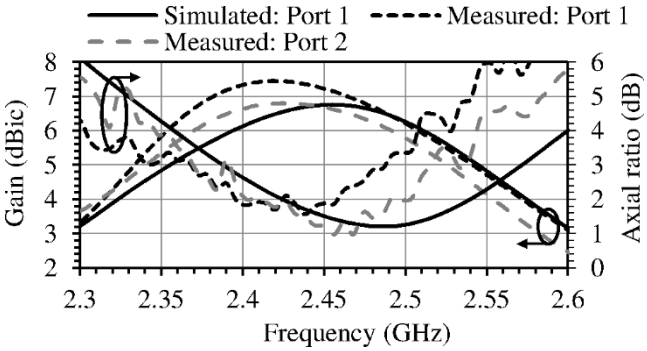

Fig. 10: Simulated and measured bore-sight gain and axial ratio over frequency.

TABLE I
COMPARISON OF DUAL-CIRCULARLY POLARIZED ANTENNAS.

Ref.	Size [λ_0]	Band. [%]	X-pol. [dB]	Gain [dBic]	F/B ratio [dB]
[1]	$0.8 \times 0.8 \times 0.125$	16	13	7	15
[12]	$0.94 \times 0.94 \times 0.189$	16	17	9	13
[13]	$0.73 \times 0.73 \times 0.067$	18	11	6	16
[14]	$0.73 \times 0.7 \times 0.013$	3.5	10	6	10
[15]	$0.5 \times 0.5 \times 0.025$	1	15	-	15
This	$0.5 \times 0.5 \times 0.057$	4	18	6	>30

REFERENCES

[1] J. Wu, H. Yang and Y. Yin, "Dual circularly polarized antenna with suspended strip line feeding," *Progress In Electromagnetic Research C*, vol. 55, pp. 9-16, 2014.

[2] M. Ramírez and J. Parrón, "Concentric annular ring slot antenna for global navigation satellite systems," *IEEE Antennas and Wireless Prop. Letters*, vol. 11, pp. 705-707, 2012.

[3] M. Qiu and G.V. Eleftheriades, "Highly Efficient Unidirectional Twin Arc-Slot Antennas on Electrically Thin Substrates," *IEEE Antennas and Wireless Prop. Letters*, vol. 52, pp. 54-58, 2004.

[4] F. Elek, R. Abhari and G.V. Eleftheriades, "A uni-directional ring-slot antenna achieved by using an Electromagnetic Band-Gap surface," *IEEE Trans. Antennas and Propagation*, vol. 53, no. 1, pp. 181-190, 2005.

[5] J. Joubert, J.C. Vardaxoglou, W.G. Whittow and J.W. Odendaal, "CPW-fed cavity-backed slot radiator loaded with an AMC reflector," *IEEE Trans. Antennas and Propagation*, vol. 60, no. 2, pp. 735-742, 2012.

[6] D. Sievenpiper, L. Zhang, R.F.J. Broas, N.G. Alexopoulos, and E. Yablonovitch, "High-impedance electromagnetic surfaces with a forbidden frequency band," *IEEE Trans. Microw. Theory Tech.*, vol. 47, no. 11, pp. 2059–2074, Nov. 1999.

[7] Z.H. Jiang, D.E. Brocker, P.E. Sieber and D.H. Werner, "A compact, low-Profile metasurface-enabled antenna for wearable medical body-area network devices," *IEEE Trans. Antennas and Propagation*, vol. 62, no. 8, pp. 4021-4030, 2014.

[8] C.Y.D. Sim, F.R. Cai and Y.P. Hsieh, "Multiband slot-ring antenna with single- and dual-capacitive coupled patch for wireless local area network/worldwide interoperability for microwave access operation," *IET Microwaves, Antennas & Propagation*, Vol. 5, no. 11, pp. 1830–1835, 2011.

[9] H. Mosallaei and K. Sarabandi, "Antenna Miniaturization and Bandwidth Enhancement Using a Reactive Impedance Substrate," *IEEE Trans. Antennas and Propagation*, Vol. 52, no. 9, pp. 2403–2414, 2004.

[10] J. Joubert and J.W. Odendaal, "Design of compact planar rat-race and branch-lne hybrid couplers using polar curves," *Microwave and Optical Tech. Letters*, vol. 57, no. 11, pp. 2637-2640, 2015.

[11] G. Mayhew-Ridgers, J.W. Odendaal and J. Joubert, "Single-layer capacitive feed for wideband probe-fed microstrip antenna elements," *IEEE Trans. Antennas and Propagation*, vol. 51, no. 6, pp. 1405-1407, 2003.

[12] C. Zhang, X. Liang, X. Bai, J. Geng and R. Jin, "A broadband dual circularly polarized patch antenna with wide beamwidth," *IEEE Antennas and Wireless Prop. Letters*, vol. 13, pp. 1457-1460, 2014.

[13] X.-Z. Lai, Z.-M. Xie, Q.-Q. Xie and X.-L. Cen, "A dual circularly polarized RFID reader antenna with wideband isolation," *IEEE Antennas and Wireless Prop. Letters*, vol. 12, pp. 1630-1633, 2013.

[14] A. Narbudowicz, X. Bao and M.J. Ammann, "Dual Circularly-Polarized Patch Antenna Using Even and Odd Feed-Line Modes," *IEEE Trans. Antennas and Propagation*, vol. 61, no. 9, pp. 4828-4831, 2013.

[15] M.T. Zhang, Y.B. Chen, Y.C. Jiao and F.S. Zhang, "Dual Circularly Polarized Antenna of Compact Structure for RFID Application," *Journal of Electromagn. Waves and Appl.*, Vol. 20, No. 14, 1895–1902, 2006.

[16] CST Microwave Studio 2015. [Online]. Available: https://www.cst.com/.